Functional Piglet Model for the Clinical Syndrome and Postmortem Findings Induced by Staphylococcal Enterotoxin B

YVONNE A. VAN GESSEL, SACHIN MANI, SHUGUANG BI, RASHA HAMMAMIEH, JEFFREY W. SHUPP, RINA DAS, GARY D. COLEMAN, AND MARTI JETT[1]

Division of Pathology, Department of Molecular Pathology, Walter Reed Army Institute of Research, Silver Spring, Maryland 20910

Staphylococcal enterotoxin (SE) B causes serious gastrointestinal illness, and intoxication with this exotoxin can lead to lethal toxic shock syndrome. In order to overcome significant shortcomings of current rodent and nonhuman primate models, we developed a piglet model of lethal SEB intoxication. Fourteen-day-old Yorkshire piglets were given intravenous SEB, observed clinically, and sacrificed at 4, 6, 24, 48, 72, or 96 hrs posttreatment. Clinical signs were biphasic with pyrexia, vomiting, and diarrhea within 4 hrs, followed by terminal hypotension and shock by 96 hrs. Mild lymphoid lesions were identified as early as 24 hrs, with severe lymphadenopathy, splenomegaly, and prominent Peyer's patches found by 72 hrs. Widespread edema—most prominent in the mesentery, between loops of spiral colon, and in retroperitoneal connective tissue—was found in animals at 72 hrs. Additional histologic changes included perivascular aggregates of large lymphocytes variably present in the lung and brain, circulating lymphoblasts, and lymphocytic portal hepatitis. Preliminary molecular investigation using gene array has uncovered several gene profile changes that may have implications in the pathophysiology leading to irreversible shock. Five genes were selected for further study, and all showed increased mRNA levels subsequent to SEB exposure. The use of this piglet model will continue to elucidate the pathogenesis of SEB intoxication and facilitate the testing of new therapeutic regimens that may better correlate with human lesions. Exp Biol Med 229:1061–1071, 2004

Key words: pigs; irreversible shock; vascular collapse; mesenteric edema; staphylococcal enterotoxin B; end-organ failure; superantigens; hypoxia; toxic shock syndrome

The staphylococcal enterotoxins (SE) are a group of pyrogenic exoproteins produced by gram-positive *Staphylococcus aureus*. Exposure to SE has been shown to initiate a range of clinical abnormalities from gastrointestinal upset to lethal toxic shock syndrome (TSS). Once introduced into host tissues, these proteins have the ability to elicit pathology in many different systems. Within 4 hrs of ingestion, SE symptoms can be documented and include vomiting, diarrhea, nausea, and abdominal pain (1). Normally enterotoxicosis abates within 24 hrs, and anorexia persists for 5–7 days.[2] Currently there are at least 12 serotypes of SE described, which are named sequentially by letter (2). Staphylococcal enterotoxin (SE) B is one of the most clinically significant and well-studied members of this family. Staphylococcal enterotoxin B is known to induce typical food poisoning symptoms, such as fever, vomiting, and diarrhea; is implicated as a potent inducer of TSS; and is a potential biological threat agent (3). Much of the lethal effects of SEB have been attributed to superantigenicity and subsequent T-cell proliferation with massive inflammatory cytokine release (4, 5).

Unlike traditional antigens, superantigens (SAgs) can stimulate up to 20% of the host's T-cell repertoire. This is accomplished by their unique ability to bypass conventional antigen processing and presentation. Extracellular SE successfully binds both MHC II on antigen-presenting cells and the T-cell receptor, creating a functional immunological synapse (6). Specifically, it has been shown that interactions with SAgs primarily involves the variable region of the TCR beta chain (5). Subsequent to proliferation, most T-cells whose cognate antigen is not present will undergo clonal deletion, resulting in immunosuppression. By contrast, in susceptible individuals activated T-cells may continue to be stimulated and exacerbate autoimmune disease (7).

Of great interest is the ability of SEB to interact with nonimmunological tissue. In the gastrointestinal tract it has

This work was supported by grants USAMRMC: seed funding (ILIR) and GX-004-04.

[1] To whom correspondence should be addressed at Department of Molecular Pathology, Walter Reed Army Institute of Research, 503 Robert Grant Avenue, Silver Spring, MD 20910. E-mail: marti.jett@na.amedd.army.mil

Received May 28, 2004.
Accepted July 22, 2004.

1535-3702/04/22910-1061$15.00

[2] Luis do Carmo et al., personal communication, May 2002.

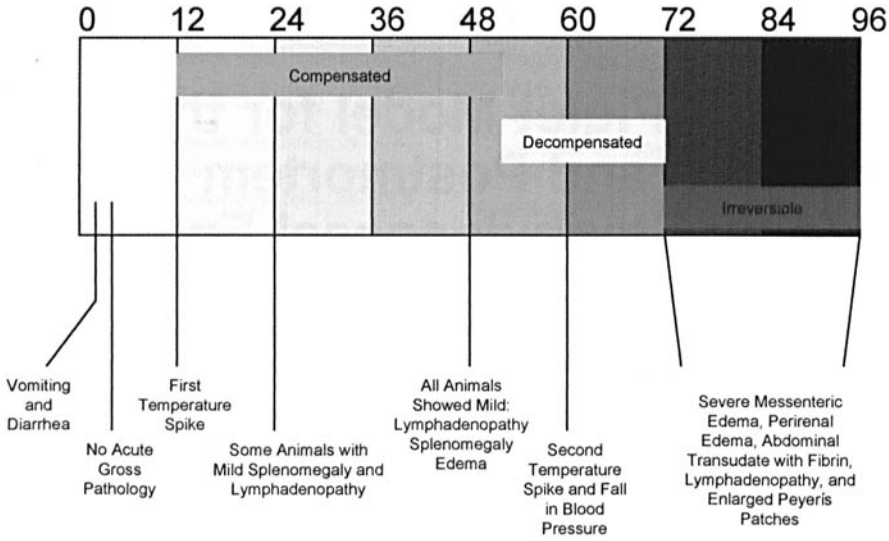

Figure 1. Chronology of staphylococcal enterotoxin B (SEB)–induced piglet toxic shock syndrome (TSS). This graphic shows vital sign changes and gross pathology associated at different time points after SEB exposure. The stages compensated, decompensated, and irreversible shock are loosely assigned to show correlation with human disease.

been shown that SEB poses the ability to bind and traverse protective intestinal epithelia (8–10). After this process of transcytosis, SEB gains access to the circulation and systemic tissue. In the kidney proximal tubule, SEB has been shown to bind galactosylceramide. This binding has potential implication in the etiology of SEB-induced hypotension and renal failure (11–13). For *in vitro* systems, SEB demonstrated marked effects on pulmonary arterial cells. Toxin exposure elicited barrier dysfunction, which occurred in the absence of effecter cells or their intermediate products (14).

Many *in vivo* systems for studying SEB have been and are currently being employed. However, this area is deficient in an effective and economic animal model, which closely parallels human staphylococcal enterotoxicosis. The nonhuman primate model (*Macaca mulatta*; Refs. 15–17) has proven to simulate SEB disease progression, but it is limited because of high cost, short supply, and complexity of animal care. Rabbit models have been developed to specifically map the lesion progression of TSS toxin-1 (TSST-1, another exotoxin produced by *S. aureus*); however, high doses are required, and they need to be introduced via continual peritoneal infusion. Multiple strains of mice have also been used as *in vivo* models for SEB. Most recently, a group of researchers has shown that C3H/HeJ mice exhibit histopathology and lethality to intranasal SEB (18). With this new exception, traditional mouse models of SEB intoxication require either genetic manipulation (19–21) or prior sensitization with D-galactosamine or endotoxin (4). Even with co-administered D-galactosamine or the newer transgenic mouse, the clinical syndrome in mice does not mimic that seen in higher order mammals.

In the present study a lethal SEB model using 14-day-old Yorkshire piglets was assessed for diagnostic parameters and relevance to human disease progression. This model could provide a promising alternative to traditional *in vivo* models for SEB. Piglets are easy to obtain, cost-efficient, and require minimal care compared with primates. This paper characterizes the clinical syndrome, histological lesions, and postmortem findings of intravenous SEB-exposed (lethal dose) piglets at varying time points.

Materials and Methods

Animals. Litters of approximately eight 12-day-old male and female Yorkshire piglets were obtained from Archer Farms (Darlington, MD) and housed in groups of approximately three piglets (assigned by treatment) in metal runs (~3 × 10 ft) lined by rubber mats. Piglets were maintained under controlled lighting (12-hour light-dark cycle) at a temperature of 85°F and humidity of ~60%. Animals were fed swine prestarter complete feed (Hubbard Feeds, Mankato, MN). Piglets had continual access to feed, water, and a 2-3 heat lamp source at one end of the run. At approximately 18 days of age, anesthetized piglets (isoflurane, 3% initially, achieving maintenance at ~1.5–2%; Abbott Labs, North Chicago, IL) received a lethal dose of SEB (150 μg/kg) or an equivalent volume of saline administered into the ear vein using a 26 g, three quarter–inch catheter. At 4, 6, 24, 48, 72, or 96 hrs posttreatment, animals were anesthetized with isoflurane, terminal measurements and blood were obtained, and the piglets were sacrificed using Buthanasia-D (Burns Biotech, Omaha, NE) administered via intracardiac injection.

Toxin Preparation. Staphylococcal enterotoxin B, lot 14-30, purified by the method of Schantz *et al.* (22), was stored as a dry powder in premeasured vacuum ampules. A working stock solution was made by dissolving the SEB in sterile pyrogen-free water to achieve a concentration of 5

mg/ml, and that solution was aliquoted and stored frozen. At the time of use, an appropriate aliquot was thawed and diluted with IV-injectable saline to 300 μg/ml. Use of SEB at 150 μg/kg was lethal to all animals tested.

Clinical Observations and Measurements. Animals were monitored continuously for clinical signs for the first 18 hrs posttreatment and every 6 hrs until sacrifice. Recorded clinical observations included piglet symptoms for at least three piglets per time period and for three different experiments (Fig. 1). Rectal body temperature was measured at least hourly 0–12 hrs and one to two times daily thereafter (Fig. 2A). Systolic blood pressure was measured by Ultrasonic Doppler Flow Detector (Model 811BL; Parks Medical Electronics, Aloha, OR; Fig. 2B).

Gross and Microscopic Pathology. After sacrifice, a complete necropsy was performed as follows: 4 hrs (one piglet), 6 hrs (one piglet), 24 hrs (five piglets), 48 hrs (five piglets), 72 hrs (seven piglets), and 96 hrs (four piglets). At least one saline control piglet was examined per litter, with a total of seven saline controls. A full set of tissues from each animal was fixed in 10% neutral buffered formalin. Fixed tissues were routinely trimmed, embedded in paraffin, sectioned at 5–7 μm, and stained with hematoxylin and eosin for microscopic examination. Tissues examined microscopically for this report were thymus, stomach, jejunum, spiral colon, descending colon, liver, spleen, pancreas, kidney, adrenal gland, urinary bladder, multiple lymph nodes, lung, heart, and brain.

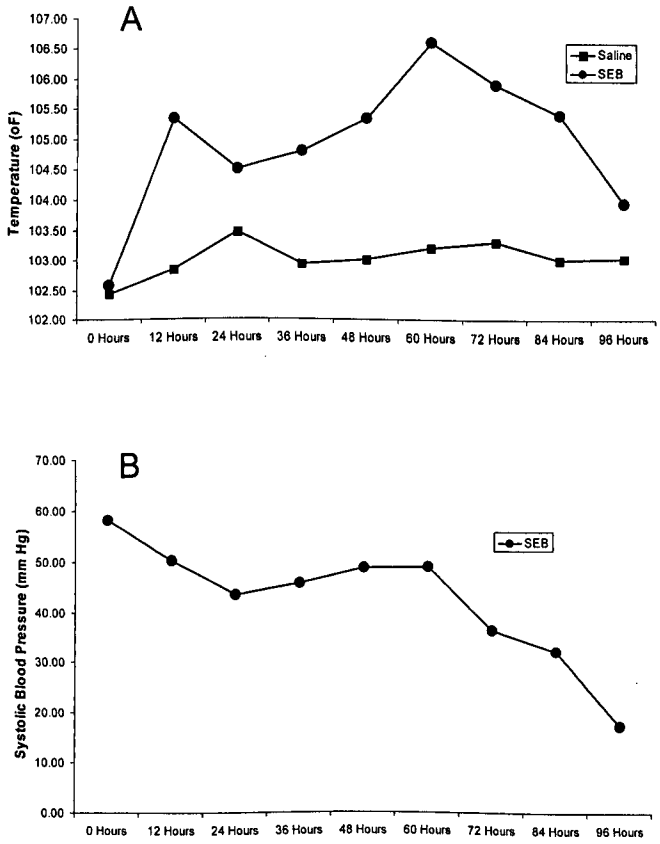

Figure 2. Vital signs. (A) Rectal body temperature measurements are shown in 12 hr intervals through 96 hrs postexposure. Each data point represents the average measurement of seven to eight animals selected from at least three separate experiments (staphylococcal enterotoxin B [SEB] = 150 μg/kg and control = equivalent volume of saline). (B) Results of systolic blood pressure measurements, using Doppler sonography, are also shown in 12-hr increments through 96 hrs postexposure. Each data point represents the mean of seven to eight animals from at least three separate experiments.

Gene Studies. Whole blood samples were collected into CPT Vacutainer tubes (BD, Franklin Lakes, NJ) at various time points and processed in accordance with the manufacturer's specifications, which allow for the enrichment of peripheral mononuclear cells (PBMC). Total RNA was subsequently isolated from PBMCs using TRIzol reagent (Life Technologies, Grand Island, NY) following manufacturer protocol.

Preliminary gene array yielded data that implicated several gene profile changes post-SEB treatment (data not shown). Five representative genes were chosen, and primer pairs to be used for PCR were designed based on known mRNA sequences (Genbank, PubMed) using Primer 3 (available at www.basic.nwu.edu) or Genelooper 2.0 from Geneharbor Inc. (Gaithersburg, MD).

Equal amounts of total RNA were reverse transcribed to cDNA using oligo $(dT)^{12\text{-}18}$and Superscript reverse transcriptase II (Invitrogen, Carlsbad, CA). The obtained cDNA was used as a template for PCR reactions using a PCR master mixture (Roche, Indianapolis, IN). Each cDNA was subjected to 25–30 PCR cycles using a GeneAmp 9600 thermal cycler (Perkin Elmer, Norwalk, CT) with conditions that resulted in a single specific amplification product of the correct size. Amplification was empirically determined to be in the linear range. All mRNA amounts were normalized relative to 18S rRNA. Reaction products (10 μl) were visualized after electrophoresis on a 1% agarose gel using SYBR Green I (Kemtek, Rockville, MD). Gels were digitized using a BioRad Molecular Imager FX (BioRad, Hercules, CA), and band intensities were used to calculate mRNA abundance.

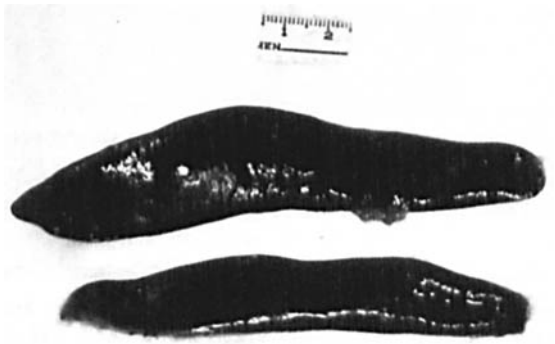

Figure 3. Mild splenomegaly. Staphylococcal enterotoxin B (SEB)–treated animals showed consistent mild splenomegaly (top) at 24 hrs as compared with control animals receiving saline (bottom).

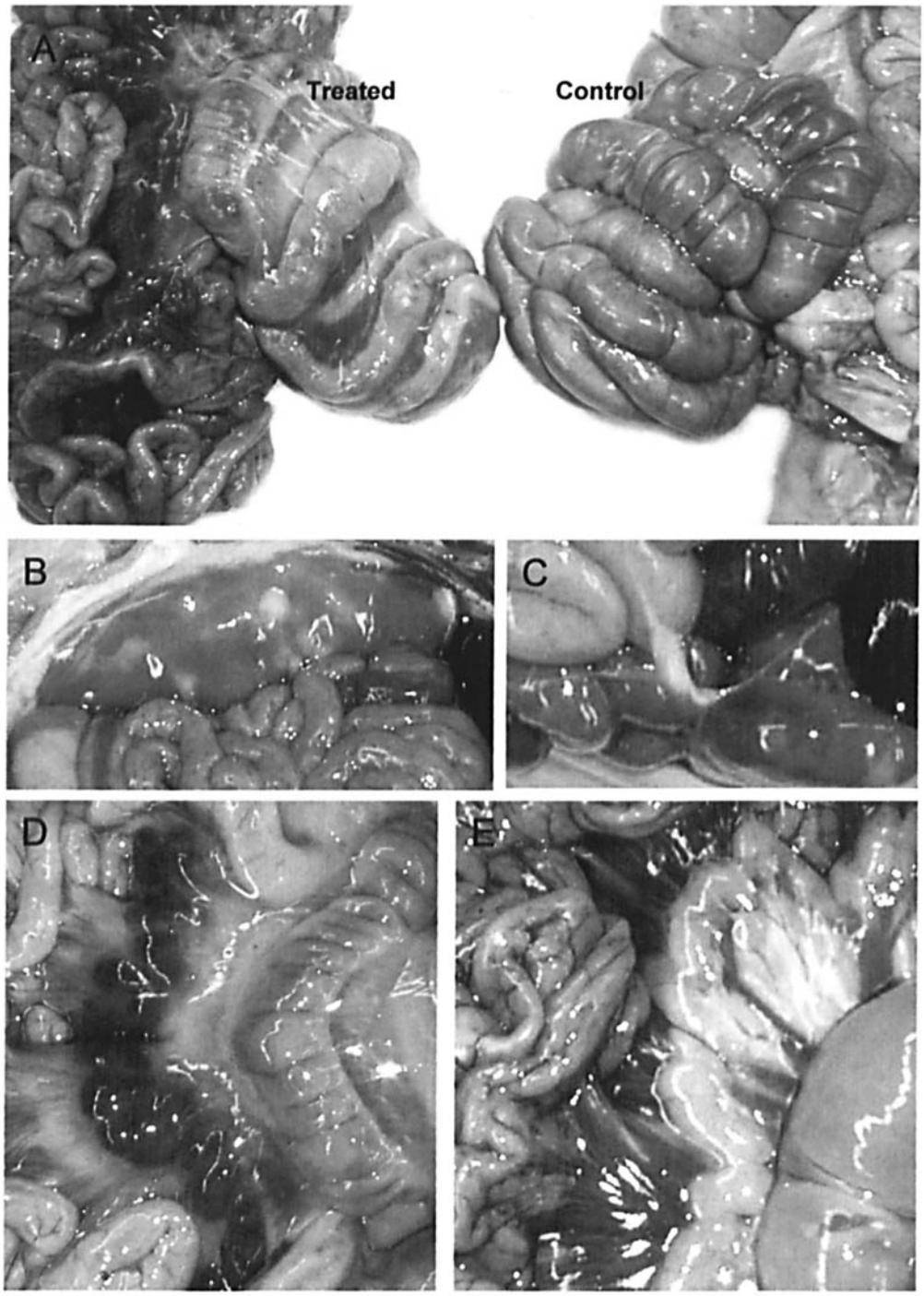

Figure 4. Gross pathology at 72–96 hrs. (A) All animals had severe mesenteric edema most prominently associated with loops of spiral colon (left) compared with saline control animals (right). (B) Perirenal edema. (C) Staphylococcal enterotoxin B (SEB)–exposed animals had marked abdominal transudate with fibrin accumulation.. Mesenteric lymphadenopathy with characteristic dark red appearance was found in all experimental animals (D) as compared with normal mesenteric lymph node presentation in control animals (E).

Results

Clinical Signs. Administration of iv SEB at 150 μg/kg was lethal (or deemed nonsurvivable by the attendant veterinarian) in 31/31 piglets. This concentration of toxin was found most effective after preliminary dose/response experiments using a range of 30–200 μg/kg. After administration of the SEB, pre-established behavioral characteristics were recorded for each animal as a function of time postexposure during the course of the experiment (continually for the first 6 hrs and intermittently during the rest of the experiment). Five descriptions of piglet behavior for each of three categories (healthy, incapacitation, prostration) were established based on observed behavior from other studies with piglets. The animals showed onset of typical incapacitation signs (transient vomiting [~3–6 episodes], severe diarrhea, anorexia) that began at 0.8–1.5

hrs postexposure (Fig. 1). The diarrhea and anorexia persisted during the remainder of the experiment. From 3–7 hrs, the animals stayed huddled together in a remote area of the cage, showing continually increasing signs of prostration. Once an animal progressed to a state of unrecoverable shock (as determined by attendant veterinarian), euthanasia was provided.

Plotted rectal temperatures showed two febrile peaks at 12 and 60 hrs, with the 60-hr time point being most extreme. Around Day 3, temperatures began to fall and showed no evidence of homeostatic recovery (Fig. 2A). Systolic blood pressures were variable throughout most of the time course; however, a distinct hypotensive trend was observed at or around the third day of observation (Fig. 2B).

Gross Findings. Gross changes were progressive over time. No significant gross changes were present in the piglets necropsied at 4 and 6 hrs post–SEB treatment or in any saline control animals. By 24 hrs, mildly enlarged mesenteric lymph nodes and mild splenomegaly were present in two of five animals (Fig. 3). By 48 hrs post–SEB treatment, all animals had consistent mild splenomegaly when compared with control animals and diffuse mild to moderate enlargement of the mesenteric lymph nodes that were often bright to dark red. Six of seven animals at this time point had mild to moderate perirenal, mesenteric, gall bladder, and gastric wall edema and mildly enlarged and congested peripheral lymph nodes. Two of the seven animals had prominent red Peyer's patches and a marked abdominal transudate with strings of fibrin.

Gross lesions were most remarkable at 72 and 96 hrs. All animals necropsied at these time periods had severe mesenteric edema that was most prominent between loops of spiral colon (Fig. 4A), as well as perirenal edema (Fig. 4B), variable edema of the gall bladder and gastric wall, and mild diffuse subcutaneous edema. This was accompanied by a marked abdominal transudate (protein, 2.5 g/dl, hypocellular) with strands of fibrin (Fig. 4C). Mesenteric lymph nodes were greatly enlarged, dark red (Fig. 4D and E), and sometimes contained multifocal white areas of necrosis.

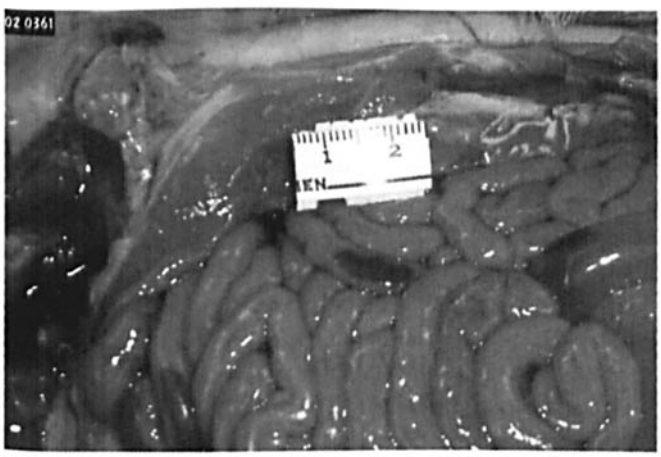

Figure 5. Congested Peyer's patches. Many animals necropsied after 72 hrs showed prominent and congested Peyer's patches.

Peripheral lymph node involvement was similar and varied from minimal to severe. Peyer's patches were often prominent and red (congested; Fig. 5).

Microscopic Findings. Histologic examination of selected tissues confirmed gross observations and helped to further characterize changes. The general progression of histologic changes in the mesenteric lymph nodes was mild lymphoid hyperplasia by 24 hrs; progression to moderate lymphoid hyperplasia and congestion by 48 hrs; and marked lymphoid necrosis with hemorrhage, edema, and fibrin accumulation by 72–96 hrs (Fig. 6A–D). Mild to moderate diffuse lymphoid hyperplasia was present in mesenteric lymph nodes in all animals examined at 24 hrs postexposure. At 48 hrs, all mesenteric lymph nodes examined had moderate to severe diffuse lymphoid hyperplasia. Many blood vessels in these nodes were congested, and the loose peripheral tissue analogous to medullary sinuses contained many free erythrocytes. In addition, there were few small scattered areas of hemorrhage and lymphoid necrosis. Lymphoid necrosis was much more extensive in six of seven and three of three mesenteric lymph nodes examined at 72 and 96 hrs, respectively. At these time points extensive lymphoid necrosis characterized by abundant karyorrhectic debris was accompanied by marked hemorrhage and edema often with fibrin lining small-caliber vessels and prominent fibrin thrombi (Fig. 6E and F). Changes in the peripheral lymph nodes were similar but much less severe and tended to occur at the later time periods.

Lymphoid hyperplasia was also present in all spleens examined at 24 hrs posttreatment and later. This change was characterized by mild diffuse expansion of the periarteriolar lymphoid sheaths (PALS; Fig. 7A and B). The lymphocytes in the affected PALS were larger, with increased cytoplasm and a large irregularly round stippled nucleus, and there were increased numbers of mitotic figures in these areas (Fig. 7C and D).

Severe mesenteric edema between loops of spiral colon seen grossly at 2 and 96 hrs (Fig. 4A) was verified histologically. Microscopically mesenteric connective tissue was loosely arranged and widely separated by a lightly eosinophilic to clear material and delicate eosinophilic fibrillar material (edema) and many extravasated red blood cells. Mesenteric lymphatics were consistently ectatic.

Additional histologic findings included lymphoblastic perivascular infiltrates and mild portal lymphoplasmacytic hepatitis. Small perivascular lymphocytic cuffs were present in the lungs of most animals examined at 48 hrs and later (five of six at 48 hrs, seven of seven at 72 hrs, and three of four at 96 hrs; Fig. 8A) and in the brain of two animals examined at 96 hrs (Fig. 8B). Cuffs often contained evidence of lymphoid necrosis with accumulation of karyorrhectic debris. Mild lymphoplasmacytic portal hepatitis (Fig. 8C–F) was variably present at 24 hrs and later: three of five piglets at 24 hrs, three of five piglets at 48 hrs, six of seven piglets at 72 hrs, and one of four piglets at 96 hrs.

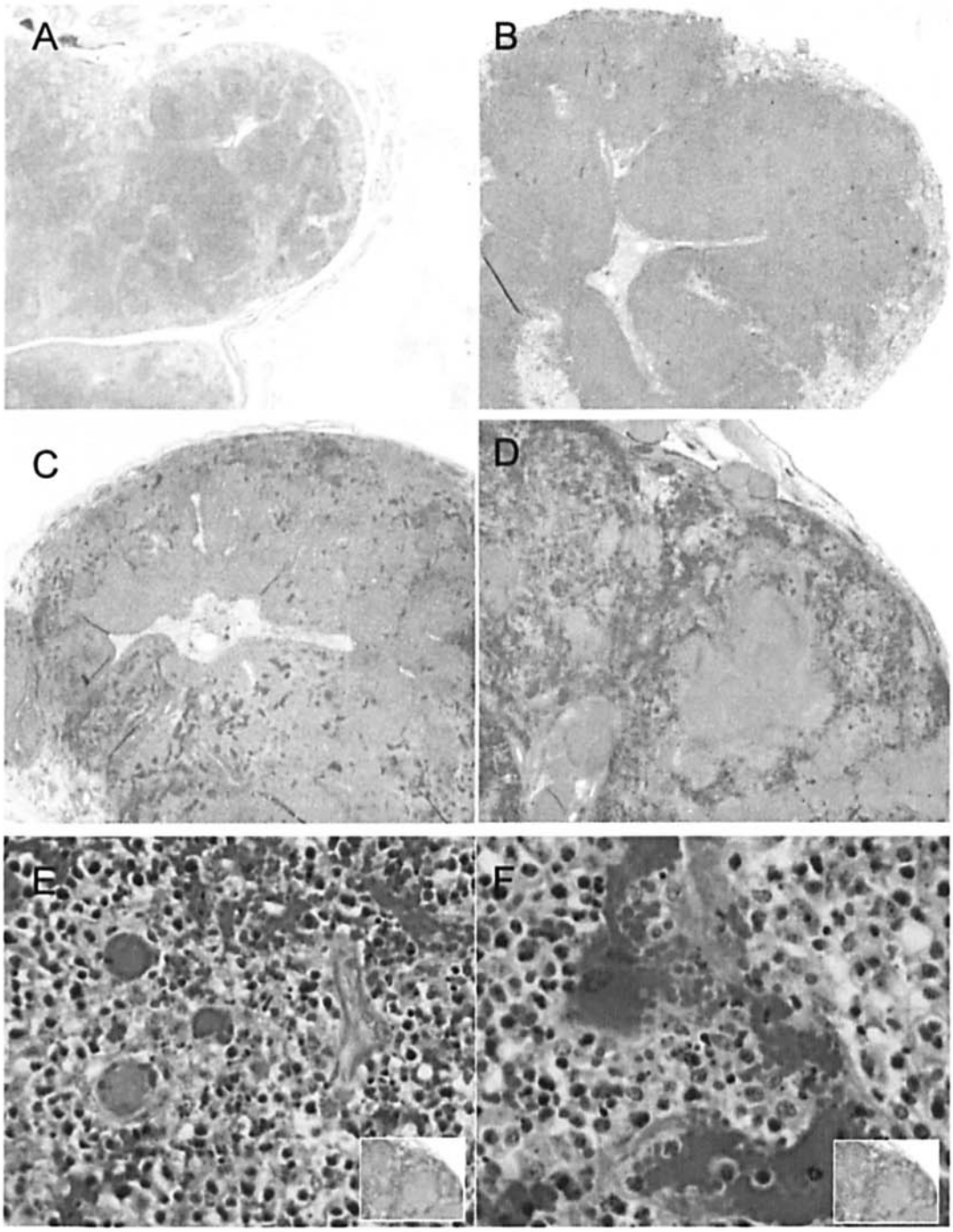

Figure 6. Lymph node histopathology. (A) Saline control mesenteric lymph node. (B–D) Mesenteric lymph node hyperplasia progression 24, 48, and 72 hrs, respectively (hematoxylin and eosin, ×10). Mesenteric lymphoid necrosis with karyorrhectic debris, hemorrhage and fibrin thrombi at 72 (E) and 96 (F) hrs (hematoxylin and eosin, ×40).

SEB-Induced Gene Changes. After initial survey using custom gene microarrays, five genes were selected for study at 2, 6, 24, 48, and 72 hrs post-SEB exposure using reverse transcription (RT)-PCR (Fig. 9). The mRNA levels for vasopressin receptor 1a (V1a), a peripheral receptor associated with vasoconstriction, were markedly increased at 24 and 72 hrs (~10-fold and ~25-fold, respectively). Interestingly, the timing of the V1a gene changes coincided with observed systolic blood pressure changes graphed in Figure 2A. Sodium, K-ATPase subunits α and β gene profiles showed a time-dependent increase, which were greatest at 48 hrs. Although both subunits followed a similar trend, the β isoform proved to have a larger increase as compared with that of the α isoform (~8-fold vs. ~2-fold at 48 hrs). Early growth response gene 1 (Egr1), a key transcription factor implicated in many disease processes including hypoxia, showed an increase at all time points. Most remarkably was an increase in mRNA levels at the 24-hr time point. Finally, the gene profile for the soluble angiotensin binding protein (sABP) was also increased at all time points with highest levels found at 48 hrs.

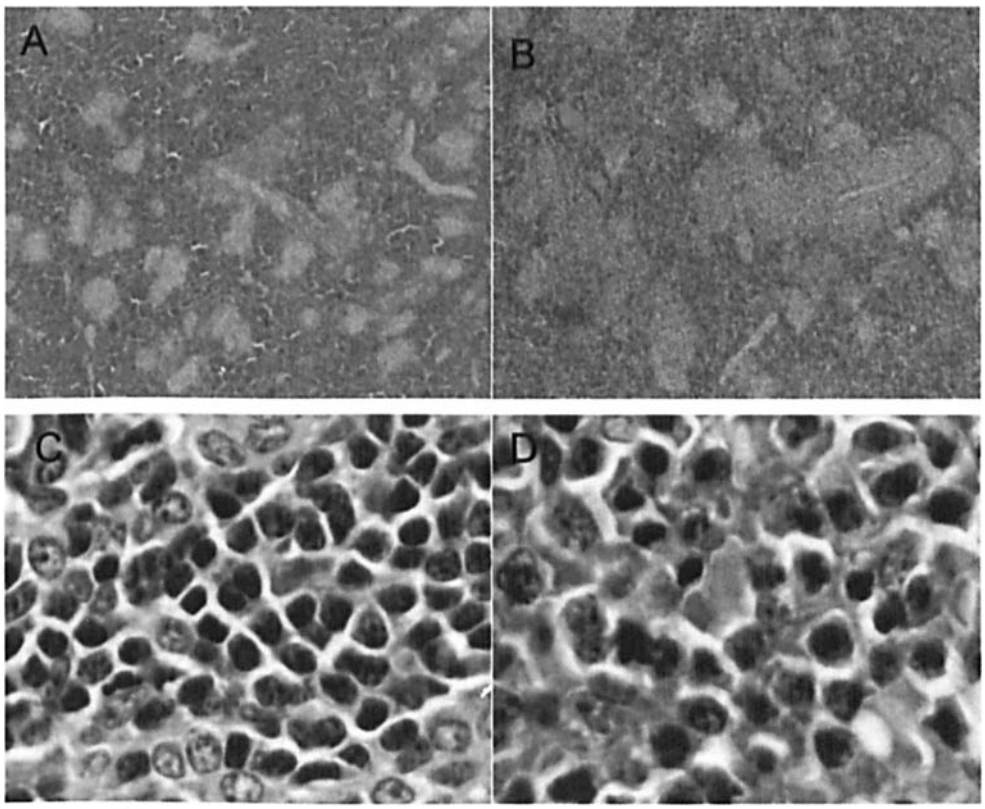

Figure 7. Splenic histopathology. Mild diffuse expansion of the periarteriolar lymphoid sheaths 24 hrs post–staphylococcal enterotoxin B (SEB) exposure (B) compared with saline control (A; hematoxylin and eosin, ×10). Enlarged lymphocytes with increased mitotic figures 24 hrs post-SEB (D) compared with saline control (C; hematoxylin and eosin, ×100).

Discussion

We have developed a clinically relevant piglet model of lethal SEB intoxication that we propose is superior to the current monkey and rodent models. This model more realistically parallels SEB intoxication in people than described mouse models, and piglets are easier to obtain, maintain, and handle than the nonhuman primate model.

This piglet model exhibits a biphasic clinical response to SEB intoxication that is virtually identical to that described in people but is not described in mouse models. Although lethal SEB intoxication has been achieved in previously manipulated mouse models, none of these models exhibit the typical initial gastrointestinal signs described in humans. In addition, the small size of these animals makes obtaining many clinical measurements such as repeat routine hematology, serum chemistries, blood pressure, and body temperature difficult.

The monkey model of lethal SEB intoxication is clinically superior to mouse models. Interestingly, the subtle clinical biphasic response to SEB intoxication shown by rhesus monkeys is not as exuberant or easily detected and monitored as that seen in this piglet model. This is likely a result of the fact that the laboratory rhesus monkey retains many behavioral characteristics of its wild counterpart, including remarkable masking of clinical disease, which increases survival under natural adverse conditions; this is in marked contrast to the domestic pig whose disposition has been markedly altered by selective breeding. In addition, working with nonhuman primates, especially rhesus macaques, comes with a unique set of limitations, most notably high expense, limited supply, and biosafety concerns. The aggressive nature of these monkeys and complications associated with Herpes B–positive colonies make heavy sedation or anesthesia necessary for many routine procedures. In contrast, the piglets used in this model are easy to obtain and relatively inexpensive. The social nature of these animals allows routine procedures to be performed without anesthesia or sedation and with minimal stress to the animal and handler.

In addition, study of other porcine models of human disease indicate that this species shows strong similarities to humans with respect to vascular responsiveness (23) and is a good model with which to study cardiovascular disease. In fact, Lee *et al.* (24) used porcine aortic endothelial cells to demonstrate that TSST-1 has a direct toxic effect on endothelium. There is also a described swine model of septic shock that culminates in a hypotensive crisis (25) that is similar to that observed in this model.

We have shown that administration of intravenous SEB to piglets results in terminal hypotension and shock similar to that seen in toxic shock syndrome in people and SEB intoxication in the rhesus macaque. Postmortem findings in people, monkeys, and piglets indicate that

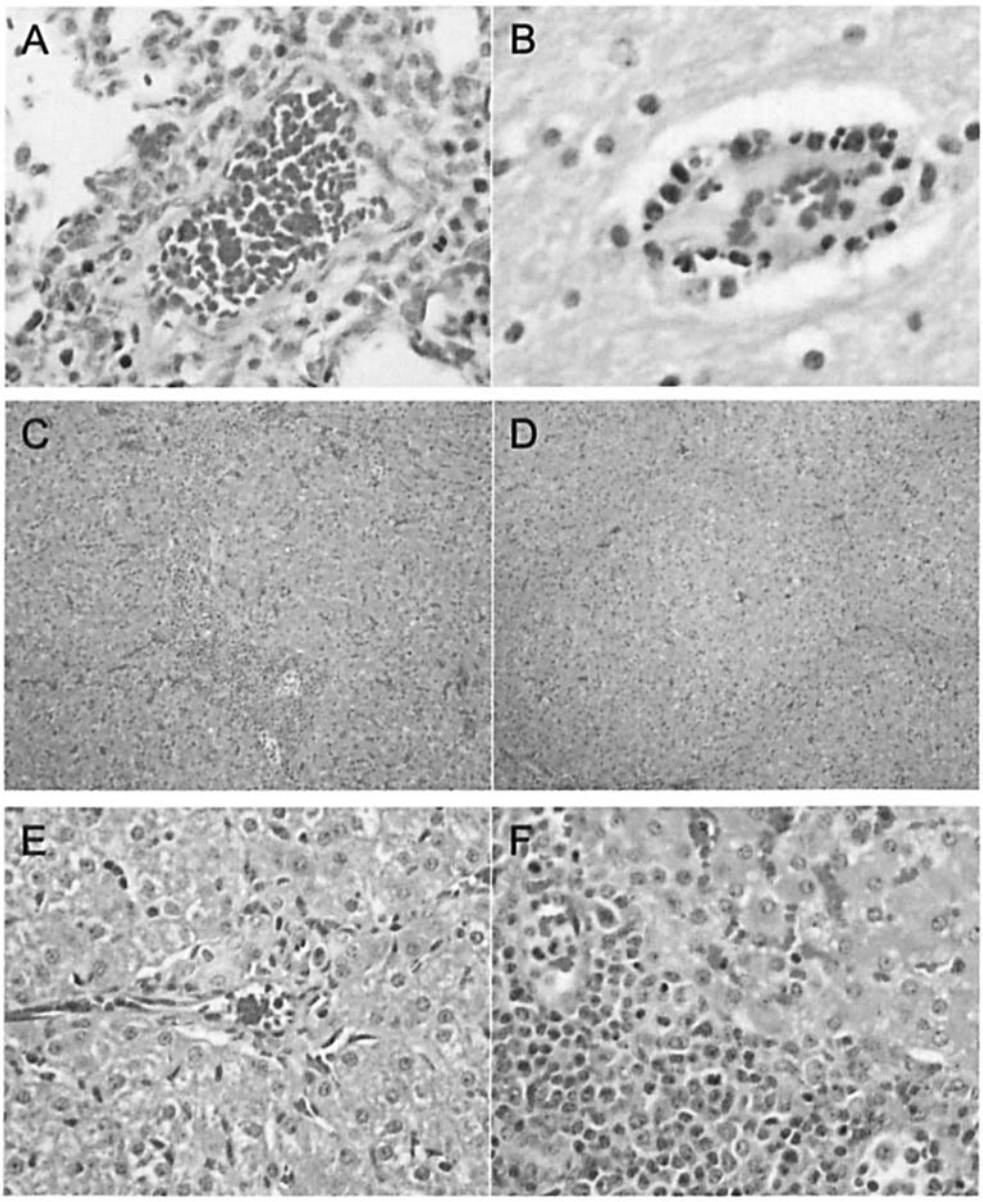

Figure 8. Pulmonary, cerebral, and hepatic histopathology. Perivascular lymphocytic cuffs present in the lungs 72 hrs post-staphylococcal enterotoxin B (SEB) exposure (A) and brain at 96 hrs (B; hematoxylin and eosin, ×40). Lymphoplasmacytic portal hepatitis (D and F) compared with control (C and E). (C–E) Stained with hematoxylin and eosin (C and D) ×10 and (E and F) ×40.

hypotension and shock in SEB intoxication is a result of leakage of fluid from vessels into extravascular spaces. Pulmonary edema is the most consistent and remarkable gross lesion associated with death in the primate model of intravascular SEB intoxication (16, 26) and in people with TSS (27). One major difference in this piglet model compared with the disease in humans is that terminal edema is predominantly focused on the abdomen, rather than the thorax, resulting in severe mesenteric and perirenal edema with comparatively minor edema at other sites. It is interesting to note that other natural and experimental angiotoxic diseases in the pig result in vascular leakage with edema predominantly in the abdominal region. In edema disease, a well characterized porcine disease, direct endothelial binding of Shiga-like toxin type IIe (SLT-IIe) secreted by *E. coli* results in marked spiral colon mesenteric edema similar to that seen in this SEB piglet model (28). In another porcine model that displays classical signs of circulatory shock, edema of the gastric wall and gall bladder is a result of experimental intravenous administration of T-2 toxin, a mycotoxin secreted by *Fusarium* species thought to cause moldy corn disease in swine (29). The abdominally focused edema in pigs may constitute a species difference that should be considered, especially in research aimed at treating late-stage hypotensive shock and pulmonary edema. However, we feel that this is still a valid model for lethal SEB pathogenesis studies and treatment trials.

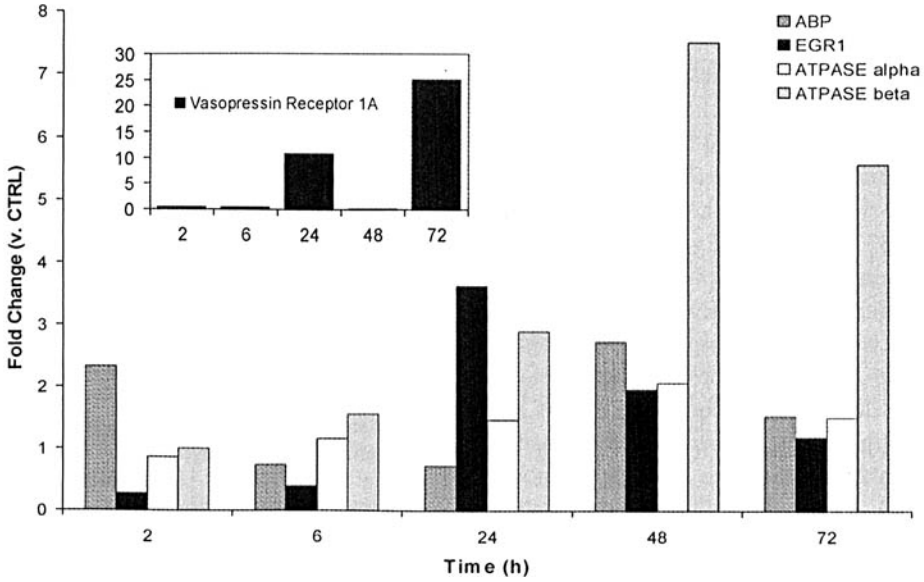

Figure 9. Staphylococcal enterotoxin B (SEB)–induced gene changes. PCR product was subjected to electrophoresis and bands were visualized using Cyber Green. Fluorescent intensity at each time was compared with that of saline control, and data are presented as fold-change. Each point represents the mean of triplicate experiments. (Standard deviations for 2, 6, 24, 48, and 72 hours are the following: V1a, 0.21, 0.29, 3.2, 0.16, and 4.8; sABP, 0.5, 0.2, 0.2, 0.4, and 0.5; *Egr*1, 0.07, 0.08, 0.22, 0.21, and 0.27; ATPase α, 0.22, 0.05, 0.30, 0.46, and 0.23; and ATPase β, 0.47, 0.99, 1.5, 2.53, and 1.8).

Another characteristic unique to swine is the unique porcine lymph node architecture. Porcine lymph nodes are essentially reversed from other mammalian lymph nodes in that lymphoid tissue is centrally located and surrounded by loose peripheral lymphoreticular tissue resembling the medullary sinuses in other species. Although porcine lymph nodes are morphologically different, the functional flow of lymph is essentially identical to other species (30) and in the author's (Y.A.V.) opinion does not represent a significant species difference.

Histological lesions in this piglet model are similar to those described in other animal models of SEB intoxication. Ulrich *et al.* (17) provides a detailed description of both pulmonary and nonpulmonary lesions associated with lethal aerosol SEB exposure in the rhesus macaque. This model also had widespread T-lymphocyte hyperplasia with enlarged lymph nodes, expanded PALS, and circulating lymphoblasts. In addition, lymphocytic portal infiltrates similar to those seen in this model were also reported in the exposed monkeys. Another report of lethal aerosol SEB-exposed monkeys described pulmonary perivascular lymphocytic infiltrates similar to those seen in this study (31). Lymphoid hyperplasia followed by lympholysis in the spleen is described in an actinomycin-D primed mouse model (21). A similar change was noted in a mouse model of aerosol SEB exposure.[3] These findings are consistent with the immunological manifestations of SAg exposure.

As in the mouse models, marked lympholysis was apparent in most piglets at 72 and 96 hrs post-SEB administration. However, this change was limited to severely affected lymph nodes and was not apparent in the thymus or spleen. It is possible that the severe lymphoid depletion noted at autopsy of several lethal cases of human TSS (27) was a sequela of massive lympholysis. As TSS is lethal only in a small percentage of cases (27), it is interesting to hypothesize that this change may be associated with lethality.

The febrile state of treated animals is of particular interest and raises many questions. Studies using staphylococcal enterotoxin A (SEA) mutants suggest that the emetic and superantigenic activity of SEs may be separate (32). Immediately following exposure, piglets presented with an emetic phase that was not associated with temperature increase. Marked temperature elevation was not recorded in animals until after the last emetic event. If superantigenic T-cell stimulation and subsequent cytokine production was solely responsible, one would suspect that the timing of emesis and fever would closely overlap. These data support the previously discerned hypothesis that the gastrointestinal and pyrogenic effects of SE may in fact be the result of a different mechanism.

The timing of clinical symptoms, vital measurements, and pathologic lesions appears to be in direct concert (Fig. 1). The initial phases of intoxication caused severe incapacitation and occurred in the absence of gross or histological pathology. Animals appeared to recover after initial onset and were left only with residual diarrhea and fever. Gross lesions appeared to develop around 24 hrs, corresponding with a further increase in body temperature. At 60 hrs animal temperatures began to fall, corresponding

[3] P.A. Vogel, personal communication, March 2003.

with incremental reductions in systolic blood pressure and marked progression of pathologic lesions.

In order to elucidate pathways responsible for SEB lesions, we have begun to profile gene changes. In this study we present data on five genes that were flagged subsequent to preliminary gene array surveying (Fig. 9). The transcription factor *Egr*1 is shown to have altered expression in the face of hypoxia (33, 34). Also, *Egr* family members have been implicated in the nonlymphoid expression of FasL and TNF (35). Interestingly, mRNA levels of *Egr*1 were highest at 24 hrs when the first signs of pathological lesions became evident. A binding protein for angiotensin, sABP, is found widely distributed in peripheral tissues and also the brain (36). Although its physiologic relevance is uncertain, sABP may play a role in the balance of smooth muscle contraction (37). V1a, unlike V2a, is recognized to initiate vasoconstriction upon binding of its ligand vasopressin (anti-diuretic hormone, ADH). This vasoconstriction is part of a large compensatory response that mobilizes in instances of hypotension. By increasing peripheral vasculature resistance, blood pressure can be returned to a level that ensures adequate tissue perfusion. In this study, V1a mRNA levels are increased notably at 24 hrs, a time when systolic blood pressure re-equilibrates, and these levels are further increased at 72 hrs in the beginning of hypotensive crisis.

The complex nature of SE pathophysiology has posed many questions scientifically, and much of the host's response to these toxins has been explained through immunology. As we progress further in understanding the chronology and severity of lesions induced by SEB, it will be necessary to further investigate the interaction of SE with nonimmunological tissue. Most notably would be the correlation of SE effects on endo and epithelia and the presence of irreversible shock.

In summary we have characterized the clinical syndrome and postmortem findings of a 14-day-old Yorkshire piglet model of lethal SEB intoxication and propose that this model is superior to previously described models. It is our hope that study of this piglet model will further elucidate the pathogenesis of SEB intoxication and enable us to test new therapeutic regimens.

We acknowledge the expert advice of COL A. Peter Vogel and Dr. Thomas Boyle, as well as the technical assistance, for various parts of this project, of Iona Brasov, Kristen Cobb, William Dahl, Hubert Pham, Kelly Gillen, Funmi Obiri, and Karen Lovelace. The views of the authors do not purport to reflect the position of the Department of the Army or the Department of Defense (Para 4-3) AR 360-5. All animal use was carried out in accordance with AR 70-18, paragraph 12.d., in compliance with the Animal Welfare Act, adhering to the principles enunciated in *The Guide for the Care and Use of Laboratory Animals.*

1. Jett M, Brinkley W, Neill R, Gemski P, Hunt R. *Staphylococcus aureus* enterotoxin B challenge of monkeys: correlation of plasma levels of arachidonic acid cascade products with occurrence of illness. Infect Immun 58:3494–3499, 1990.
2. Jarraud S, Peyrat MA, Lim A, Tristan A, Bes M, Mougel C, Etienne J, Vandenesch F, Bonneville M, Lina G. egc, a highly prevalent operon of enterotoxin gene, forms a putative nursery of superantigens in Staphylococcus aureus. J Immunol 166:669–677, 2001.
3. Marrack P, Kappler J. The staphylococcal enterotoxins and their relatives [erratum, Science 248:1066, 1990]. Science 248:705–711, 1990.
4. Miethke T, Wahl C, Heeg K, Echtenacher B, Krammer P, Wagner H. T-cell–mediated lethal shock triggered in mice by the superantigen staphylococcal enterotoxin B: critical role of tumor necrosis factor. J Exp Med 175:91–98, 1992.
5. Johnson HM, Torres BA, Soos JM. Superantigens: structure and relevance to human disease. Proc Soc Exp Biol Med 212:99–109, 1996.
6. Jardetzky TS, Brown JH, Gorga JC, Stern LJ, Urban RG, Chi YI, Stauffacher C, Strominger JL, Wiley DC. Three-dimensional structure of a human class II histocompatibility molecule complexed with superantigen. Nature 368:711–718, 1994.
7. Johnson HM, Russell JK, Pontzer CH. Staphylococcal enterotoxin microbial superantigens. Faseb J 5:2706-2712, 1991.
8. Hamad AR, Marrack P, Kappler JW. Transcytosis of staphylococcal superantigen toxins. J Exp Med 185:1447–1454, 1997.
9. Shupp JW, Jett M, Pontzer CH. Identification of a transcytosis epitope on staphylococcal enterotoxins. Infect Immun 70:2178–2186, 2002.
10. McKay DM, Singh PK. Superantigen activation of immune cells evokes epithelial (T84) transport and barrier abnormalities via IFN-gamma and TNF alpha: inhibition of increased permeability, but not diminished secretory responses by TGF-beta2. J Immunol 159:2382–2390, 1997.
11. Chatterjee S, Khullar M, Shi WY. Digalactosylceramide is the receptor for staphylococcal enterotoxin-B in human kidney proximal tubular cells. Glycobiology 5:327–333, 1995.
12. Chatterjee S, Jett M. Glycosphingolipids: the putative receptor for *Staphylococcus aureus* enterotoxin-B in human kidney proximal tubular cells. Mol Cell Biochem 113:25–31, 1992.
13. Normann SJ. Renal fate of staphylococcal enterotoxin B. Lab Invest 25:126–132, 1971.
14. Campbell WN, Fitzpatrick M, Ding X, Jett M, Gemski P, Goldblum SE. SEB is cytotoxic and alters EC barrier function through protein tyrosine phosphorylation *in vitro*. Am J Physiol 273:L31–L39, 1997.
15. Normann SJ, Jaeger RF, Johnsey RT. Pathology of experimental enterotoxemia. The *in vivo* localization of staphylococcal enterotoxin B. Lab Invest 20:17–25, 1969.
16. Stiles JW, Denniston JC. Response of the rhesus monkey, *Macaca mulatta*, to continuously infused staphylococcal enterotoxin B. Lab Invest 25:617–625, 1971.
17. Ulrich RG, Sidell S, Taylor TJ, Wilhelmsen CL, Franz DR. Staphylococcal enterotoxin B and related pyrogenic toxins. In: Sidell FR, Takafuji ET, Franz DR, eds. Textbook of Military Medicine. Part I: Warfare, Weaponry , and the Casualty. Medical Aspects of Chemical and Biological Warfare. Washington, DC: Office of the Surgeon General, pp621–630, 1997.
18. Savransky V, Rostapshov V, Pinelis D, Polotsky Y, Korolev S, Komisar J, Fegeding K. Murine lethal toxic shock caused by intranasal administration of staphylococcal enterotoxin B. Toxicol Pathol 31:373–378, 2003.
19. Anderson MR, Tary-Lehmann M. Staphylococcal enterotoxin-B-induced lethal shock in mice is T-cell–dependent, but disease susceptibility is defined by the non–T-cell compartment. Clin Immunol 98:85–94, 2001.
20. Yeung RS, Penninger JM, Kundig T, Khoo W, Ohashi PS, Kroemer G, Mak TW. Human CD4 and human major histocompatibility complex class II (DQ6) transgenic mice: supersensitivity to superantigen-induced septic shock. Eur J Immunol 26:1074–1082, 1996.

21. Chen JY, Qiao Y, Komisar JL, Baze WB, Hsu IC, Tseng J. Increased susceptibility to staphylococcal enterotoxin B intoxication in mice primed with actinomycin D. Infect Immun 62:4626–4631, 1994.
22. Schantz EJ, Roessler WG, Wagman J, Spero L, Dunnery DA, Bergdoll MS. Purification of staphylococcal enterotoxin B. Biochemistry 4:1011–1016, 1965.
23. Feletou M, Teisseire B. Vascular pharmacology of the micropig: importance of the endothelium. In: Swindle MM, Moody DC, Phillips LD, Eds. Swine As Models in Biomedical Research. Ames: Iowa State University Press, pp74–95, 1992.
24. Lee PK, Vercellotti GM, Deringer JR, Schlievert PM. Effects of staphylococcal toxic shock syndrome toxin 1 on aortic endothelial cells. J Infect Dis 164:711–719, 1991.
25. Hoban LD, Paschall JA, Eckstein J, Nadkari V, Lee CR, Williams TJ, Reusch D, Nevola JJ, Carcillo JA. Awake porcine model of intraperitoneal sepsis. In: Swindle MM, Moody DC, Phillips LD, Eds. Swine As Models in Biomedical Research. Ames: Iowa State University Press, pp246–264, 1992.
26. Finegold MJ. Interstitial pulmonary edema. An electron microscopic study of the pathology of staphylococcal enterotoxemia in Rhesus monkeys. Lab Invest 16:912–924, 1967.
27. Larkin SM, Williams DN, Osterholm MT, Tofte RW, Posalaky Z. Toxic shock syndrome: clinical, laboratory, and pathologic findings in nine fatal cases. Ann Intern Med 96:858–864, 1982.
28. Gelberg HB. Alimentary system. In: McGavin MD, Carltom WW, Zachary JF, Eds. Thomson's Special Veterinary Pathology (3rd ed.). St. Louis: Mosby, pp42–43, 2001.
29. Pang VF, Lorenzana RM, Beasley VR, Buck WB, Haschek WM. Experimental T-2 toxicosis in swine. III. Morphologic changes following intravascular administration of T-2 toxin. Fundam Appl Toxicol 8:298–309, 1987.
30. Landsverk T. Immune system. In: Dellmann D, Eurell JA, Eds. Textbook of Veterinary Histology (5th ed.). Baltimore: Williams & Wilkins, pp137–142, 1998.
31. Mattix ME, Hunt RE, Wilhelmsen CL, Johnson AJ, Baze WB. Aerosolized staphylococcal enterotoxin B-induced pulmonary lesions in rhesus monkeys (*Macaca mulatta*). Toxicol Pathol 23:262–268, 1995.
32. Hoffman M, Tremaine M, Mansfield J, Betley M. Biochemical and mutational analysis of the histidine residues of staphylococcal enterotoxin A. Infect Immun 64:885–890, 1996.
33. Jin K, Mao XO, Eshoo MW, del Rio G, Rao R, Chen D, Simon RP, Greenberg DA. cDNA microarray analysis of changes in gene expression induced by neuronal hypoxia in vitro. Neurochem Res 27:1105–1112, 2002.
34. Ten VS, Pinsky DJ. Endothelial response to hypoxia: physiologic adaptation and pathologic dysfunction. Curr Opin Crit Care 8:242–250, 2002.
35. Droin NM, Pinkoski MJ, Dejardin E, Green DR. Egr family members regulate nonlymphoid expression of Fas ligand, TRAIL, and tumor necrosis factor during immune responses. Mol Cell Biol 23:7638–7647, 2003.
36. Hagiwara H, Sugiura N, Wakita K, Hirose S. Purification and characterization of angiotensin-binding protein from porcine liver cytosolic fraction. Eur J Biochem 185:405–410, 1989.
37. Webb RC, Kiron MA, Rosenberg E, Soffer RL. Antiserum to angiotensin-binding protein inhibits vascular responses to angiotensin II. Am J Physiol 255:H1542–H1544, 1988.